Optimization of thickness uniformity of coatings on spherical substrates using shadow masks in a planetary rotation system

Jian Sun (孙 建)[1,2], Weili Zhang (张伟丽)[1*], Kui Yi (易 葵)[1], and Jianda Shao (邵建达)[1]

[1] *Key Lab. of Materials for High Power Laser, Shanghai Institute of Optics and Fine Mechanics, Chinese Academy of Sciences, Shanghai 201800, China*

[2] *University of Chinese Academy of Sciences, Beijing 100049, China*

[*] *Corresponding author: wlzhang@siom.ac.cn*

Received January 16, 2014; accepted March 5, 2014; posted online April 30, 2014

A model is developed to improve thickness uniformity of coatings on spherical substrates rapidly and automatically using fixed shadow masks in a planetary rotation system. The coating thickness is accurately represented by a function composed of basic thickness, self-shadow effect, and shadow mask function. A type of mask with parabolic contours is proposed, and the thickness uniformity of coatings on spherical substrates can be improved in a large range of ratios of clear aperture (CA) to radius of curvature (RoC) by optimizing shadow masks using a numerical optimization algorithm. Theoretically, the thickness uniformity improves to more than 97.5% of CA/RoC from –1.9 to 1.9. Experimentally, the thickness uniformities of coatings on a convex spherical substrate (CA/RoC = 1.53) and on a concave spherical substrate (CA/RoC=–1.65) improve to be better than 98.5% after corrected by the shadow masks.

OCIS codes: 310.0310, 310.6805, 310.1860.

doi: 10.3788/COL201412.053101.

Imaging optics requirements for numerous optical systems involve pushing design and manufacturing objectives to high numerical aperture (NA). High-NA optical systems typically require numerous elements, some of which have steep convex or concave spherical surfaces[1]. Normally, uniform coatings deposited on these elements are required to provide constant optical properties over the optic surfaces. If not properly corrected, the nonuniform thickness profiles will seriously affect the image quality[2]. Therefore, controlling thickness uniformity of coatings is crucial in the application of these strongly curved spherical optical components.

Numerous methods have been developed to improve coating thickness uniformity, including employing simple or planetary rotation stages, using shadow masks or just modifying planetary rotation motion[3–11]. Typically, planetary rotation systems produce more uniform coatings than simple rotation systems, but they cannot achieve sufficient thickness uniformity of coatings on strongly curved spherical substrates without shadow masks[4]. Conventionally, rotating or fixed shadow masks are used in planetary rotation systems to selectively block the deposition plume, thus improving the thickness uniformity[4–7]. Fixed-position masking is the preferred method because it has the lowest-maintenance and the highest mechanical reliability.

In this letter, an accurate model is developed to improve thickness uniformity of coatings on spherical substrates rapidly and automatically in a large range of ratios of clear aperture (CA) to radius of curvature (RoC) in a planetary rotation system by designing fixed shadow masks with parabolic contours. Theoretically, the thickness uniformity improves to more than 97.5% of CA/RoC from –1.9 to 1.9. Experimentally, the thickness uniformities of coatings on a convex spherical substrate (CA/RoC = 1.53) and on a concave spherical substrate (CA/RoC = –1.65) improve to more than 98.5%, agreeing with the theoretical values.

Figure 1 shows the basic geometric configuration of the planetary rotation system with a convex substrate with CA and RoC. The source $S(x_s, y_s, z_s)$ is parallel to the planet which has a height H. The substrate is placed at the center of the planet and the CA plane maintains the same height as the planet. For a concave spherical substrate, similar configuration is applied and the RoC is a negative value. R is the radius of the planetary orbit; α is the angular position of the planet in its orbit; $P(x, y, z)$ is a surface element of the substrate; $\mathbf{c}$ is the vector from P to the center of the sphere $O(x_o, y_o, z_o)$, which has a length of RoC; L is the horizontal distance from P to O, which determines the radial position of P on the substrate; β is the initial angular position of P on the substrate in the horizontal plane, which determines the circumferential position of P on the substrate; $\mathbf{s}$ is the unitary vector of the source normal and $\mathbf{r}$ is the vector from source S to P; ϕ is the angle between $\mathbf{s}$ and $\mathbf{r}$, namely the evaporation angle; θ is the angle between $\mathbf{c}$ and $\mathbf{r}$, namely the deposition angle. The basic thickness function of coatings deposited on the surface element P is expressed as[8]

$$t = A\frac{\cos^n \phi \cos\theta}{r^2}, \tag{1}$$

where t is the film thickness, A is a constant, r is the length of vector $\mathbf{r}$, and $\mathbf{n}$ is an emission characteristic parameter of the source, which can be determined by comparing the calculated and experimental thickness distribution when no shadow mask is applied.

 © 2014 Chinese Optics Letters

For the geometrical configurations of the planetary rotation system and a spherical substrate shown in Fig. 1, the expression can be converted to coordinate geometry

$$r = |\mathbf{r}| = \sqrt{(x - x_s)^2 + (y - y_s)^2 + (z - z_s)^2}, \tag{2}$$

$$\cos\phi = \frac{\mathbf{r}\cdot\mathbf{s}}{|\mathbf{r}|\cdot|\mathbf{s}|} = \frac{z - z_s}{r}, \tag{3}$$

$$\cos\theta = (-1)^M \frac{\mathbf{r}\cdot\mathbf{c}}{|\mathbf{r}|\cdot|\mathbf{c}|} = \frac{(x-x_s)(x_o-x)+(y-y_s)(y_o-y)+(z-z_s)(z_o-z)}{r\cdot RoC}, \tag{4}$$

where M is used to distinguish convex and concave substrates (0 for convex substrates and 1 for concave substrates). The motions of center O and the element P will form the paths, which can be expressed as

$$\begin{cases} x_o = R\sin\alpha \\ y_o = R\cos\alpha \\ z_o = H + (-1)^M\sqrt{\mathrm{RoC}^2 - \mathrm{CA}^2/4} \end{cases}, \tag{5}$$

$$\begin{cases} x = R\sin\alpha + L\sin(K\alpha+\alpha+\beta) \\ y = R\cos\alpha + L\cos(K\alpha+\alpha+\beta) \\ z = H+(-1)^M(\sqrt{\mathrm{RoC}^2-\mathrm{CA}^2/4}-\sqrt{\mathrm{RoC}^2-L^2}) \end{cases}, \tag{6}$$

with limit $L \in [0, \mathrm{CA}/2]$ and $\beta \in [0, 2\pi]$. K is the teeth ratio between the solar and planet gears. Afterward, the film thickness in Eq. (1) is obtained by integration of the angular position α. That is,

$$t(L,\beta) = \int_0^{2\pi F} t(L,\beta,\alpha)\mathrm{d}\alpha, \tag{7}$$

where F is the circle number of planetary revolution.

The film thickness depends on the deposition angle of arrival molecules with respect to the substrate normal. For convex spherical substrates, when the deposition angle is larger than 90°, no arrival molecule accumulates at the point of the substrate, as shown in Fig. 2(a). For concave spherical substrates, the situation is more complicated because the region where the deposition angle is larger than 90° will shade another region, as shown in Fig. 2(b). Thus, a correcting function of the self-shadow effect $E(L,\beta,\alpha)$ is added. For a convex spherical substrate, the function is defined as

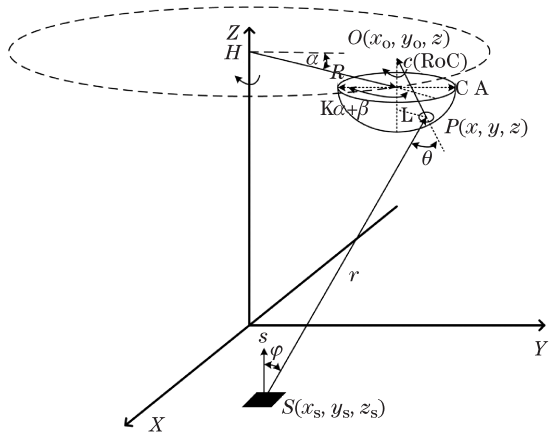

Fig. 1. Basic geometric configuration of a planetary rotation system with a convex substrate.

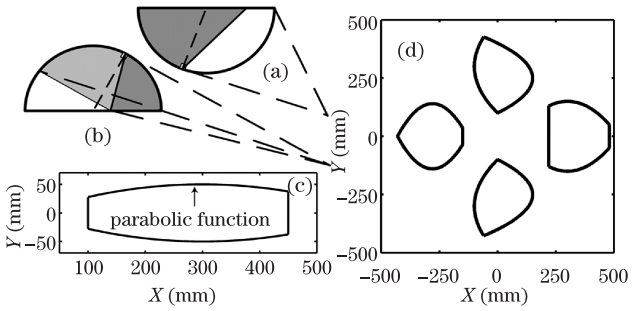

Fig. 2. Self-shadow effect of (a) a convex and (b) a concave spherical substrates. (c) A typical shadow mask with parabolic contours; (d) a typical geometric configuration of four masks fixed in the chamber.

$$E(L,\beta,\alpha) = \begin{cases} 1, & \theta \leqslant 90^\circ \\ 0, & \theta > 90^\circ \end{cases}. \tag{8}$$

For a concave spherical substrate, when the projection of the straight line connecting the element P and the source S is inside the CA, the molecules can arrive at the substrate. By contrast, no evaporated molecules accumulate at P. The coordinates (x_b, y_b, z_b) of the point B on the straight line when $z_b = H$ can be given by

$$\begin{cases} x_b = (x - x_s)(H - z_s)/(z - z_s) + x_s \\ y_b = (y - y_s)(H - z_s)/(z - z_s) + y_s \end{cases}, \tag{9}$$

The distance between B and the center of the CA whose coordinates are (x_O, y_O, H) can be calculated as

$$d = \sqrt{(x_b - x_o)^2 + (y_b - y_o)^2}, \tag{10}$$

Thus, the correcting function for a concave spherical substrate can be defined as

$$E(L,\beta,\alpha) = \begin{cases} 1, & d \leq \mathrm{CA}/2 \\ 0, & d > \mathrm{CA}/2 \end{cases}, \tag{11}$$

The film thickness function Eq. (7) can be modified as

$$t(L,\beta) = \int_0^{2\pi F} t(L,\beta,\alpha)E(L,\beta,\alpha)\mathrm{d}\alpha, \tag{12}$$

Once a stable deposition system has been configured, the thickness non-uniformity can be removed through the use of fixed shadow masks. For spherical substrates, precisely fitting the curvature of the substrate with the shadow masks is difficult, so the use of a projection diaphragm is recommended. If a horizontal plane mask is positioned at height $z_m = H_m$, the relationships that define the projection mask profile are given by

$$\begin{cases} x_m = (x - x_s)(z_m - z_s)/(z - z_s) + x_s \\ y_m = (y - y_s)(z_m - z_s)/(z - z_s) + y_s \end{cases}, \tag{13}$$

where (x_m, y_m, z_m) are the coordinates of point K having the same height as the mask on the straight line connecting the element P on the substrate and the source S.

The shape and the position of the masks can be optimized using a shadow mask function $N(L,\beta,\alpha)$ and the molecules will be blocked by the masks if the point K is inside the masks. Thus, the thickness function Eq. (12) can be modified as

$$t(L,\beta)=\int_0^{2\pi F} t(L,\beta,\alpha)E(L,\beta,\alpha)N(L,\beta,\alpha)\mathrm{d}\alpha, \quad (14)$$

The primary concern is uniform film thickness, so the thickness will be normalized, resulting in

$$t(L,\beta)=\frac{\int_0^{2\pi F} t(L,\beta,\alpha)E(L,\beta,\alpha)N(L,\beta,\alpha)\mathrm{d}\alpha}{\int_0^{2\pi F} t(0,0,\alpha)E(0,0,\alpha)N(0,0,\alpha)\mathrm{d}\alpha}\times 100\%, \quad (15)$$

Finally, a merit function can be established as

$$\text{Merit}=\sum_{L=0}^{\mathrm{CA}/2}\sum_{\beta=0}^{2\pi}\left(\frac{2t(L,\beta)}{t_{\max}(L,\beta)+t_{\min}(L,\beta)}-100\%\right)^2, \quad (16)$$

where $t_{\max}(L,\beta)$ and $t_{\min}(L,\beta)$ is the maximum and minimum relative thickness, respectively. For a given deposition system and a substrate, the masks can be derived by the minimization of the merit function by successive iterations using simulated annealing optimization algorithm with the software Matlab.

To achieve optimum merit, the initial shape of the mask is essential. A type of mask with parabolic contours is chosen because it is be most effective in improving film thickness uniformity of strongly curved spherical substrates. Figure 2(c) shows a typical geometric configuration of this mask. The profile can be defined with a parabolic function as

$$y_{\text{mask}}=a_1(x_{\text{mask}}+a_2)^2+a_3 \quad x_{\text{mask}}\in[a_4,a_5]. \quad (17)$$

Then the shape and the position of the mask can be derived by optimizing the parameters (a_1,a_2,a_3,a_4,a_5) in the function and the height of the masks H_m rapidly and automatically.

Typically, several masks are simultaneously needed. These masks have different parabolic contours that allow more parameters to be optimized, resulting in better uniform coating thickness. Inexperienced researchers also can get excellent results by try the initial parameters more times and larger ranges of the parameters. Four masks symmetrically positioned in the coating chamber like the example shown in Fig. 2(d) are preferred in our work which can be applied to various convex and concave spherical substrates, even those with strongly curved surfaces and the processing and installation were relatively simple.

The shadow mask design model is evaluated with optical coatings prepared with a commercial evaporation system (Leybold Optics SYRUSpro 1110) with a flat planetary rotation system in an 1100-mm-diameter vacuum chamber. The geometric parameters of the coatings machine are $H=730$ mm, $R=300$ mm, and $K=131/19$. The coordinates of two similar boat sources are $(-230,165,0)$ and $(-230,-165,0)$ for aluminum fluoride (AlF_3) and lanthanum fluoride (LaF_3), respectively. A convex spherical substrate holder (RoC = 128 mm, CA = 196 mm, CA/RoC = 1.53) and a concave spherical substrate holder (RoC = −127 mm, CA= 210 mm, CA/RoC=−1.65) with evenly distributed wedge-shaped quartz substrates with 15 mm in diameter along the radial direction are prepared. Single-layer AlF_3 thin films and anti-reflection (AR) coatings at 193 nm with AlF_3 and LaF_3 are fabricated to verify the uniformity of film thickness. Film thicknesses on the quartz substrates are derived from the near normal reflectance spectra obtained through a Perkin-Elmer Lambda 1050 UV/VIS/NIR spectrometer in nitrogen atmosphere using envelope method with a film analysis software Essential Macleod, representing the film thickness distribution on the substrate holders[12]. Before deposition, the vacuum chamber is pumped down to a base pressure of less than 2.7×10^{-4} Pa by a cryopump and heated to 300 °C. The deposition rates are 0.15 and 0.05 nm/s for AlF_3 and LaF_3 films, respectively.

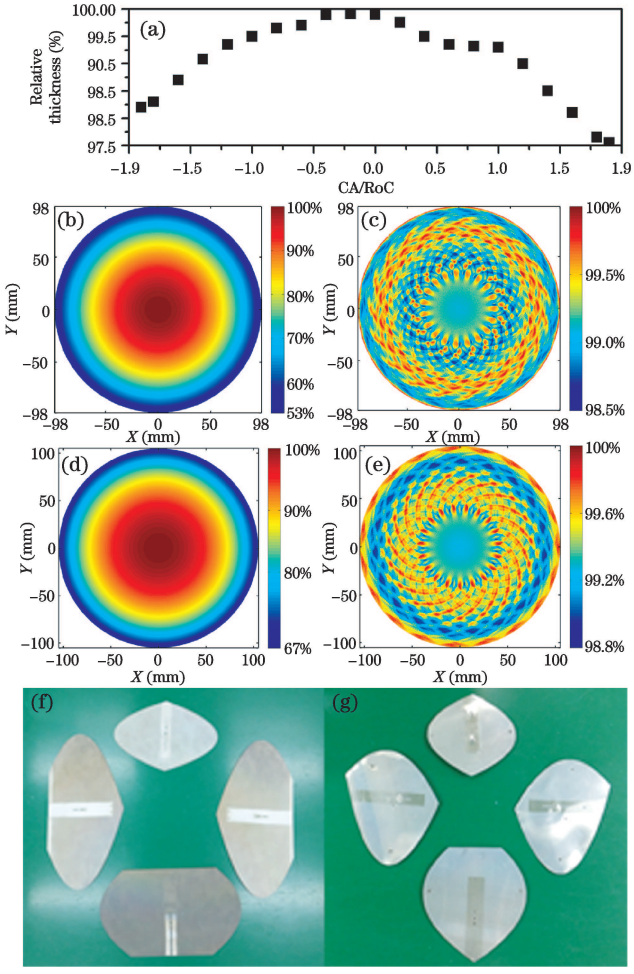

Fig. 3. (a) Theoretical relative thicknesses of coatings on spherical substrates with CA=200 mm and different CA/RoC with shadow masks; theoretical relative thicknesses of coatings on the convex spherical substrate (RoC=128 mm, CA=196 mm) (b) without and (c) with shadow masks and on the concave spherical substrate (RoC=–127 mm, CA=210 mm); (d) without and (e) with shadow masks; shadow masks for (f) the convex and (g) the concave substrate.

By fitting the calculated data and the experimental film thicknesses on the convex substrate holder when no mask is applied, the emission characteristic parameters of the evaporation sources are determined to be 2±0.2 for both AlF_3 and LaF_3. Then, shadow masks are designed for spherical substrates with CA=200 mm and different CA/RoC using this model. Figure 3(a) shows the calculated relative coating thickness with shadow masks. The thickness uniformity improves to more than 97.5% for spherical substrates with CA/RoC from –1.9 to 1.9, proving that the shadow mask design model is effective in improving coating thickness in a large range of CA/RoC.

Finally, shadow masks are designed and fabricated for the convex and concave substrate holders mentioned above. The calculated thickness uniformity on the convex spherical substrate improves from 53% to 98.5% by using the shadow masks as shown in Figs. 3(b) and (c). For the concave substrate, the calculated thickness uniformity improves from 67.8% to 98.8% as shown in Figs. 3(d) and (e). Figures 3(f) and (g) show the masks for the convex and the concave substrate.

Figures 4(a) and (b) show the measured reflectance spectra of the AlF_3 films on the Φ 15 mm fused quartz substrates at different locations along the radial direction of the convex and concave substrate holders, respectively. The spectra almost overlap, indicating that excellent uniformity is achieved. The experimental thickness uniformities of single AlF_3 films improve to more than 98.9% and 99.1% for the convex and concave substrate, respectively. The experimental thickness uniformities were a little better than the theoretical values. The difference may be caused by limited positions chosen to place the Φ 15 mm substrates on the substrate holder, measurement

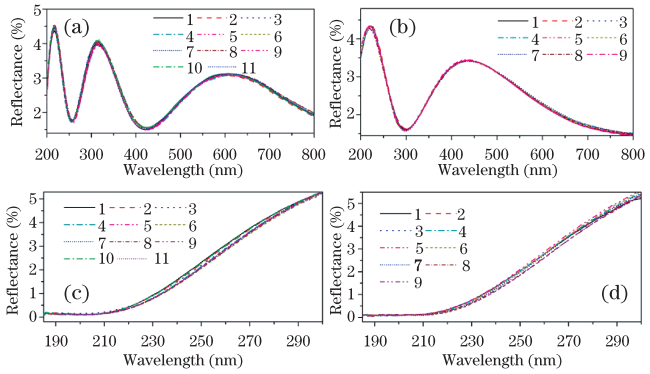

Fig. 4. Reflectance of AlF_3 films on (a) the convex spherical substrate and (b) the concave spherical substrate; reflectance of AR coatings on (c) the convex spherical substrate and (d) the concave spherical substrate.

error of the geometry of the coating machine, machining and positioning errors of the shadow masks and the substrate holders, the measurement errors of the spectra and the calculation errors of the film thickness, and so on. Figures 4(c) and (d) show the reflectance spectra of the AR coatings on the Φ 15 mm fused quartz substrates at different locations of the convex and concave substrate holders, respectively. The reflectance spectra match each other closely, especially in the anti-reflection wavelength range, indicating the validity of the shadow masks.

In conclusion, an accurate model is developed to improve thickness uniformity of coatings on spherical substrates rapidly and automatically in a planetary rotation system by designing the fixed shadow masks. A type of shadow mask with parabolic contours is proposed for optimization, which is effective in improving thickness uniformity of coatings on spherical substrates in a large range of ratios of CA/RoC. Theoretically, the thickness uniformity improves to more than 97.5% of CA/RoC from –1.9 to 1.9. Experimentally, the thickness uniformities of AlF_3 films on the convex spherical substrate (CA/RoC=1.53) and on the concave spherical substrate (CA/RoC=–1.65) improve to more than 98.5%. The reflectance spectra of the AR coatings on the substrates at different locations match each other closely, indicating the validity of this model.

References

1. P. Kelkar, B. Tirri, R. Wilklow, and D. Peterson, Proc. SPIE **7067,** 070608 (2008).
2. H. J. Qi, M. P. Zhu, W. L. Zhang, K. Yi, H. B. He, and J. D. Shao, Chin. Opt. Lett. **10,** 013104 (2012).
3. M. Gross, S. Dligatch, and A. Chtanov, Appl. Opt. **50,** C316 (2011).
4. C. Guo, M. D. Kong, C. D. Liu, and B. C. Li, Appl. Opt. **52,** B26 (2013).
5. C. D. Liu, M. D. Kong, C. Guo, W. D. Gao, and B. C. Li, Opt. Express **20,** 23790 (2012).
6. J. B. Oliver and D. Talbot, Appl. Opt. **45,** 3097 (2006).
7. F. Villa, A. Martinez, and L. E. Regalado, Appl. Opt. **39,** 1602 (2000).
8. F. Villa and O. Pompa, Appl. Opt. **38,** 695 (1999).
9. C. Liu, C. Guo, M. Kong, and B. Li, Chin. Opt. Lett. **11,** S10213 (2013).
10. Y. Q. Hou, H. J. Qi, K. Yi, and J. D. Shao, Chin. Opt. Lett. **11,** 103101 (2013).
11. P. G. Antal and R. Szipocs, Chin. Opt. Lett. **10,** 053101 (2012).
12. R. Swanepoel, J. Phys. E Sci. Instrum. **16,** 1214 (1983).